Doping-driven Mott transition in $La_{1-x}Sr_xTiO_3$ via simultaneous electron and hole doping of t_{2g} subbands as predicted by LDA+DMFT calculations

A. Liebsch
Institut für Festkörperforschung, Forschungszentrum Jülich, 52425 Jülich, Germany
(Received 5 February 2008; published 12 March 2008)

The insulator to metal transition in $LaTiO_3$ induced by La substitution via Sr is studied within multiband exact diagonalization dynamical mean field theory at finite temperatures. It is shown that weak hole doping triggers a large interorbital charge transfer, with simultaneous electron and hole doping of t_{2g} subbands. The transition is first order and exhibits phase separation between insulator and metal. In the metallic phase, subband compressibilities become very large and have opposite signs. Electron doping gives rise to an interorbital charge flow in the same direction as hole doping. These results can be understood in terms of a strong orbital depolarization.

DOI: 10.1103/PhysRevB.77.115115 PACS number(s): 71.30.+h, 71.10.Fd, 71.27.+a

I. INTRODUCTION

The remarkable sensitivity of the electronic and magnetic properties of transition metal oxides to small changes of parameters such as temperature, pressure, or impurity concentration has attracted wide attention during recent years.[1] A phenomenon of particular interest is the filling-controlled metal insulator transition in the vicinity of integer occupancies of partially filled valence bands. For instance, $LaTiO_3$ is known to be a Mott insulator which becomes metallic if La is replaced by a few percent of Sr ions.[2,3] Similarly, Ca_2RuO_4 is a Mott insulator which becomes metallic if Ca is substituted by small amounts of Sr.[4]

Theoretically, the doping-driven Mott transition has been investigated within single-band models[5–14] or multiband models based on identical subbands.[15–18] To our knowledge, only one calculation for nonequivalent subbands exists so far.[19] On the other hand, it has recently been demonstrated that orbital degrees of freedom play a crucial role in the Mott transition of materials consisting of nonequivalent partially occupied subbands. For example, whereas cubic $SrVO_3$ ($3d^1$ configuration) is metallic, isoelectronic $LaTiO_3$ exhibits a Mott transition because noncubic structural distortions lift the degeneracy among t_{2g} subbands.[20] Local Coulomb interactions strongly enhance this orbital polarization, so that the electronic structure of the insulating phase consists of a single nearly half-filled band split into lower and upper Hubbard peaks and two nearly empty t_{2g} subbands. Similarly, the monoclinic symmetry of the Mott insulator V_2O_3 ($3d^2$) yields a pair of nearly half-filled subbands (with lower and upper Hubbard peaks) and a single nearly empty t_{2g} band.[21,22] Also, the insulating phase of the layered perovskite Ca_2RuO_4 ($4d^4$) consists of a fully occupied t_{2g} band of predominant d_{xy} character and two half-filled $d_{xz,yz}$-like bands.[23,24] In view of the nearly complete orbital polarization of the Mott phase, it is evidently necessary to go beyond single-band models or multiband models for identical subbands to describe the effect of doping in these materials.

In the present work, we investigate the destruction of the Mott phase of $LaTiO_3$ due to replacement of small amounts of La by Sr. Whereas in models based on equivalent subbands doping naturally modifies all subbands in the same way, we show here that the interplay between orbital and charge degrees of freedom yields a completely different picture: The addition of only a few percent of holes to the t_{2g} bands triggers a substantially larger interorbital charge rearrangement, with a strong flow of electrons from the nearly half-filled subband toward the nearly empty ones. In other words, weak "external" hole doping of the t_{2g} bands causes a much larger "internal" simultaneous electron and hole doping of different subbands. Thus, the density-driven insulator to metal transition in $La_{1-x}Sr_xTiO_3$ is accompanied by a significant reduction of orbital polarization. Similar depolarization effects can be expected to occur in other multiband transition metal oxides.

To account for local Coulomb interactions among the Ti $3d$ electrons, we use finite temperature dynamical mean field theory (DMFT)[25] combined with exact diagonalization (ED).[26] It was recently shown[27] that this method can be generalized to multiband materials by computing only those excited states of the impurity Hamiltonian, which are within a narrow range above the ground state, where the Boltzmann factor provides the convergence criterion. Exploiting the sparseness of the Hamiltonian, these states can be computed very efficiently by using the Arnoldi algorithm.[28] Higher excited states enter via Green's functions which are evaluated using the Lanczos method. This approach is highly useful for the study of strong correlations in transition metal oxides.[24,27,29,30] Since it does not suffer from sign problems, the full Hund exchange including spin-flip and pair-exchange contributions can be taken into account. Also, relatively large Coulomb energies and low temperatures can be reached.

As shown by Pavarini *et al.*,[20] the orthorhombic lattice of $LaTiO_3$ implies that the t_{2g} density of states is not diagonal within the $d_{xy,xz,yz}$ basis. It is nonetheless possible to construct from these orbitals another basis, denoted here as a_g, e_g', which is nearly diagonal.[31] The corresponding densities of states obtained from *ab initio* calculations within the local density approximation (LDA) are shown in Fig. 1. The details of these distributions, and the 200 meV crystal field splitting between the a_g and nearly degenerate e_g' components, reflect the hybridization among $d_{xy,xz,yz}$ orbitals. The subband occupancies per spin band in the absence of correlation effects are $n_{a_g} \approx 0.23$ and $n_{e_g'} \approx 0.135$. The tetragonal

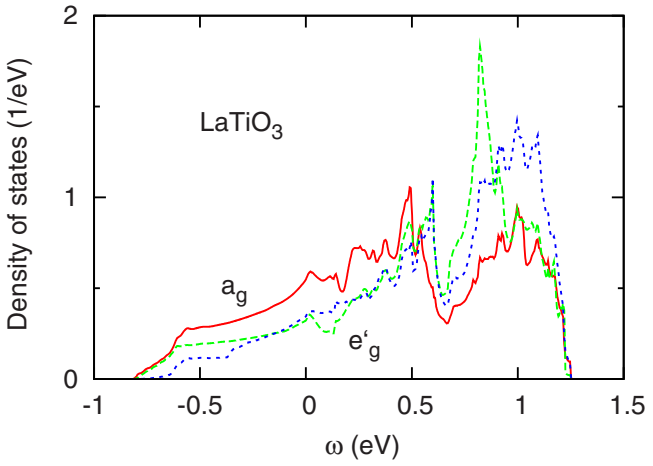

FIG. 1. (Color online) LDA density of states components of $LaTiO_3$ in nearly diagonal subband representation (Ref. 31). Solid curve: a_g states; dashed curves: e_g' states; $E_F=0$.

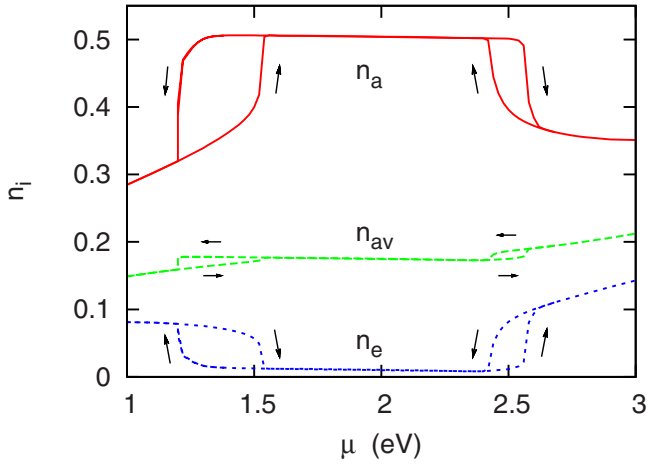

FIG. 2. (Color online) DMFT a_g and e_g' subband occupancies (per spin band) of $LaTiO_3$ as functions of chemical potential. Also shown is the average occupancy $n_{av}=(n_{a_g}+2n_{e_g'})/3$. The arrows mark the hystereses for increasing and/or decreasing μ.

crystal field splitting compares well with recent experimental estimates based on x-ray studies.[32]

In our ED scheme, each of the three a_g, e_g' orbitals couples to two or three bath levels, giving a cluster size $n_s=9$ or $n_s=12$. Since local Coulomb and exchange interactions couple the baths of the impurity orbitals, the level spacing between states is very small and finite size effects are much smaller than for a single impurity level coupled to only two or three bath levels. Hybridization between a_g, e_g' orbitals is very small. We therefore neglect nondiagonal density components in this basis, so that local quantities such as the impurity Green's function and self-energy are also diagonal in this representation. Also, the small difference between the e_g' densities is omitted and their average density is used instead. The cluster Hamiltonian is given by

$$H=\sum_{m\sigma}(\varepsilon_m-\mu)n_{m\sigma}+\sum_{k\sigma}\varepsilon_k n_{k\sigma}+\sum_{mk\sigma}V_{mk}[c_{m\sigma}^{+}c_{k\sigma}+\text{H.c.}]$$
$$+\sum_{m}Un_{m\uparrow}n_{m\downarrow}+\sum_{m<m'\sigma\sigma'}(U'-J\delta_{\sigma\sigma'})n_{m\sigma}n_{m'\sigma'}$$
$$-\sum_{m\neq m'}J[c_{m\uparrow}^{+}c_{m\downarrow}c_{m'\downarrow}^{+}c_{m'\uparrow}+c_{m\uparrow}^{+}c_{m\downarrow}^{+}c_{m'\uparrow}c_{m'\downarrow}],$$

where $\varepsilon_{m=1,\ldots,3}$ and $\varepsilon_{k=4,\ldots,n_s}$ are the impurity and bath levels, respectively, V_{mk} the hybridization matrix elements, and μ is the chemical potential. U, U', and J are the on-site Coulomb and exchange energies, with $U'=U-2J$. Only paramagnetic phases are considered. For further details see Ref. 27.

II. RESULTS

Figure 2 shows the charge transfer among a_g, e_g' bands as a function of chemical potential, where we assume $U=5$ eV and $J=0.65$ eV.[20] The temperature $T\approx 20$ meV. As in previous work,[5–19] we assume the primary effect of weak doping to be caused by the change of band filling. Hole doping is seen to occur for $\mu<1.5$ eV, electron doping for $\mu>2.5$ eV. Because of the insulating gap, the charge compressibility $\kappa=\partial n/\partial\mu$ vanishes in the intermediate range occupancies. The small deviations from $n_{a_g}=0.5$ and $n_{e_g'}=0$ in this region presumably are due to the finite temperature and ED finite size effects. The hysteresis loops near $\mu=1.5$ eV and $\mu=2.5$ eV demonstrate that the hole and electron driven Mott transitions at finite T are first order. Phase separation, where an insulating solution with $n=2n_{a_g}+4n_{e_g'}=1$ coexists with a metallic solution for $n\neq 1$, is seen to occur at both transitions. Moreover, the compressibility gets very large as the upper and lower critical values of μ at both hysteresis loops are approached.

Note that the hysteresis behavior of the a_g, e_g' subbands is much more pronounced than that of the average t_{2g} charge. Also, the subband compressibilities $\kappa_i=\partial n_i/\partial\mu$ have opposite signs and their absolute values are much larger than the average t_{2g} compressibility. These results indicate that the combined effect of charge and orbital degrees of freedom leads to a nontrivial generalization of the one-band picture close to half-filling[5–14] and of the multiband picture based on equivalent orbitals.[15–18] In the latter case, all bands exhibit the same weak hysteresis behavior as the average charge.

The unexpected and striking feature of these results is that the charge rearrangement among t_{2g} orbitals is much larger than the number of holes induced via La→Sr substitution. For instance, for $x=0.05$ ($n=0.95$), the total a_g occupancy (both spins) changes from near unity at $U=5$ eV to 0.64, whereas the total e_g' occupancy (four spin bands) changes from near zero to 0.31. Thus, the internal charge transfer from a_g to e_g' bands is six times larger than the external charge transfer due to doping with Sr. Clearly, the destruction of the Mott phase of $LaTiO_3$ via hole doping does not proceed via approximately equal participation of all subbands. Instead, weak external hole doping generates a much larger simultaneous electron and hole doping in different subbands. The physical reason for this effect is the fact that the subband compressibilities become extremely large upon crossing the first-order phase boundary between insulator and metal. Since they have opposite signs, small variations

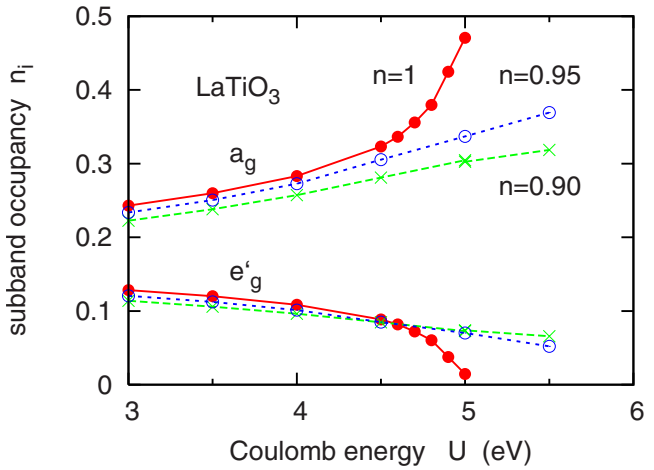

FIG. 3. (Color online) Subband occupancies (per spin band) of $La_{1-x}Sr_xTiO_3$ as functions of the Coulomb energy calculated within ED/DMFT. Solid dots: $3d^1$ ($x=0$); empty dots: $3d^{0.95}$ ($x=0.05$); crosses: $3d^{0.90}$ ($x=0.1$).

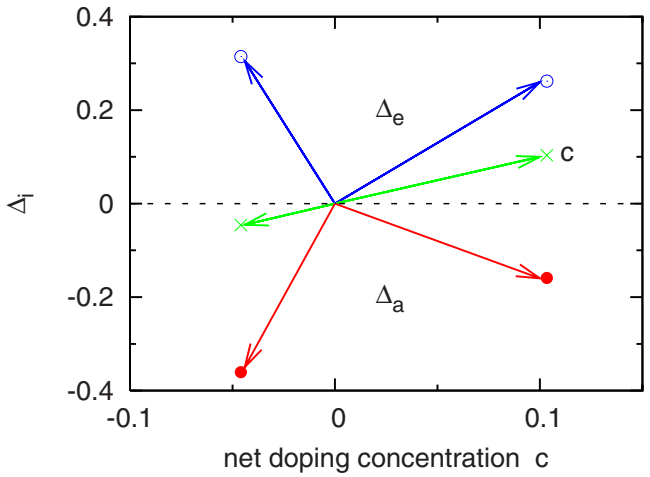

FIG. 4. (Color online) Solid and empty dots: doping induced change of total a_g and e'_g subband occupancies, Δ_a and Δ_e, respectively, for hole doping ($c\approx-0.05$, left points) and electron doping ($c\approx0.1$, right points); $U=5$ eV. In both cases, the subband doping is much larger than the net doping c indicated by the crosses.

of the chemical potential yield large variations in n_{a_g} and $n_{e'_g}$. The destruction of the $n=1$ insulator is therefore accompanied by a sudden, large charge redistribution between a_g and e'_g orbitals, with partial filling of the nearly empty e'_g states at the expense of the nearly half-filled a_g states.

This interorbital charge rearrangement is illustrated in more detail in Fig. 3 which shows the variation of the a_g, e'_g subband occupancies with the Coulomb energy for fixed total $3d$ charge. Integer and noninteger occupancies reveal qualitatively different behaviors. For $n=1$, local Coulomb interactions gradually suppress orbital fluctuations up to $U\approx4.5$ eV. In the subsequent narrow range up to $U\approx5$ eV, the a_g band is rapidly becoming nearly half-filled and the two e'_g bands nearly empty. This result supports the picture in Refs. 20 and 31 obtained via quantum Monte Carlo DMFT, where for $U=5$ eV, Ising exchange, and $T=100$ meV, $LaTiO_3$ was found to be a Mott insulator, with nearly empty e'_g subbands, and the half-filled a_g band splits into lower and upper Hubbard peaks.

For hole doping with $n=0.95$ and 0.90, on the other hand, the situation is very different: Orbital polarization increases smoothly with increasing Coulomb energy, without any sign of the critical behavior that is characteristic of the pure La compound. Evidently, the suppression of orbital fluctuations near $U=5$ eV is associated with the first-order phase transition for integer occupancy of the t_{2g} bands.

These results differ qualitatively from those in Ref. 19 obtained via DMFT based on iterated perturbation theory for nonequivalent t_{2g} subbands. For pure $LaTiO_3$, orbital polarization was found to slightly decrease from the metallic to the insulating phase, in contrast to the opposite trend discussed above and in Ref. 20. Thus, the doping induced depolarization shown in Fig. 3 is absent. At present, we have no explanation for this difference between the IPT and ED/DMFT treatments.

Since the density of states of $LaTiO_3$ is not symmetric and the t_{2g} occupation is far from one-half, it is interesting to consider also the case of electron doping, for example, via substituting La by Zr. Because the a_g band is nearly full, one might expect the donated electrons to populate the nearly empty e'_g bands, with little other changes. As for hole doping, we find a very different picture. For example, for 0.10 electron doping, 0.26 electron is injected into the e'_g bands and 0.16 holes into the a_g band. Thus, the actual number of electrons transferred to the e'_g bands is considerably larger than externally supplied. Of course, this can only be achieved via simultaneous hole doping of the a_g band.

These results are illustrated in Fig. 4 which shows the total electronic charge injected into the e'_g bands ($\Delta_e=4n_{e'_g}>0$) and the total hole charge injected into the a_g band ($\Delta_a=2n_{a_g}-1<0$) for net doping concentrations $c\approx-0.05$ and $c\approx0.1$, where $c=\Delta_a+\Delta_e=n-1$. Both electron and hole dopings are seen to cause a strong orbital depolarization, implying an internal charge flow between t_{2g} bands, which greatly exceeds the number of carriers supplied externally. Note also the lack of symmetry between electron and hole dopings.

Finally, to make contact with the photoemission data for $La_{1-x}Sr_xTiO_3$,[3] we show in Fig. 5 the spectral distributions for $n=1$ ($x=0$) and $n=0.95$ ($x=0.05$). For simplicity, we give here the ED cluster spectra which can be evaluated directly at real ω, without requiring extrapolation from the Matsubara frequencies. At integer occupancy, the system is insulating. The excitation gap is formed between the lower Hubbard peak of the a_g band and the empty e'_g bands, in agreement with Ref. 31. The hole doped system, on the other hand, is metallic, with conduction states stemming from both a_g and e'_g bands. If we associate the peak near E_F with coherent states, the large peak at 1.1 eV binding energy, i.e., below the bottom of the LDA density of states, represents the incoherent weight related to the lower Hubbard band. It has mainly a_g character, with weak e'_g admixture. The position of this feature is in good agreement with the photoemission spectra for $La_{0.95}Sr_{0.05}TiO_3$.[3] Moreover, the ratio between incoherent and coherent weights is roughly 3:1. This is also consistent with the photoemission data which reveal substantially more incoherent than coherent emission.

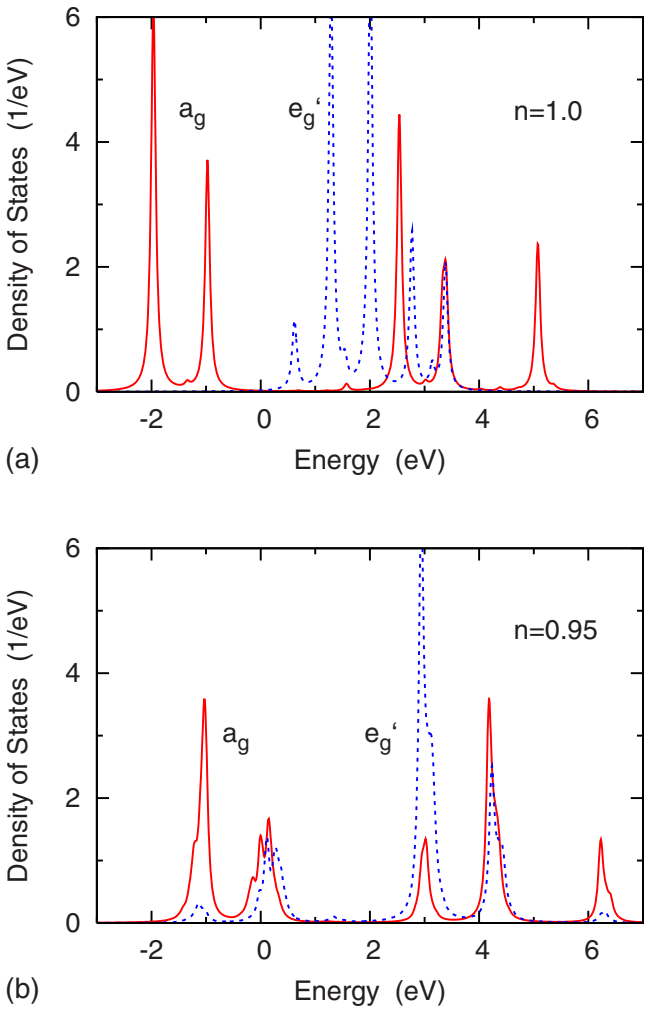

FIG. 5. (Color online) ED/DMFT spectral distributions of insulating $LaTiO_3$ (upper panel) and metallic $La_{0.95}Sr_{0.05}TiO_3$ (lower panel) for $U=5$ eV. Solid (dashed) curves: a_g (e_g') states; $E_F=0$.

It would be interesting to experimentally verify these predictions, in particular, the combined a_g, e_g' nature of the quasiparticle peak near E_F and the predominantly a_g character of the lower Hubbard band in the doped material. As shown in Fig. 3, this orbital decomposition differs markedly from the one in the insulating phase of pure $LaTiO_3$.

III. CONCLUSION

We have studied the combined effect of charge and orbital degrees of freedom on the density-driven Mott transition in $La_{1-x}Sr_xTiO_3$. The key result is that the transition from insulator to metal induced by weak doping is accompanied by a striking interorbital charge rearrangement. Thus, injection of only a few percent of holes into the Ti t_{2g} bands via doping with Sr causes a much larger simultaneous electron and hole doping of different subbands. This effect can be understood in terms of the nearly singular subband charge compressibilities which have opposite signs. The insulator to metal transition is first order and exhibits separation between insulating and metallic phases. Doping of the Mott phase therefore induces a pronounced orbital depolarization, i.e., a strong reduction of the nearly complete orbital polarization that occurs at integer occupancy. Since other multiband Mott insulators such as V_2O_3 and Ca_2RuO_4 also exhibit orbital polarization, it is likely that doping these systems with electron or hole donors will lead to a similar enhancement of orbital fluctuations as discussed here for $La_{1-x}Sr_xTiO_3$.

ACKNOWLEDGMENTS

I would like to thank Eva Pavarini for the density of states shown in Fig. 1 and Theo Costi for useful discussions. I also thank Luis Craco for comments.

[1] M. Imada, A. Fujimori, and Y. Tokura, Rev. Mod. Phys. **70**, 1039 (1999).
[2] A. Bzowski and T. K. Sham, Phys. Rev. B **48**, 7836 (1993).
[3] T. Yoshida, A. Ino, T. Mizokawa, A. Fujimori, Y. Taguchi, T. Katsufuji, and Y. Tokura, Europhys. Lett. **59**, 258 (2002).
[4] S. Nakatsuji and Y. Maeno, Phys. Rev. Lett. **84**, 2666 (2000); Phys. Rev. B **62**, 6458 (2000).
[5] N. Furukawa and M. Imada, J. Phys. Soc. Jpn. **60**, 3604 (1991).
[6] T. Pruschke, D. L. Cox, and M. Jarrell, Phys. Rev. B **47**, 3553 (1993).
[7] D. S. Fisher, G. Kotliar, and G. Moeller, Phys. Rev. B **52**, 17112 (1995).
[8] G. Kotliar, S. Murthy, and M. J. Rozenberg, Phys. Rev. Lett. **89**, 046401 (2002).
[9] Y. Ono, R. Bulla, A. Hewson, and M. Potthoff, Eur. Phys. J. B **22**, 283 (2002).
[10] A. Camjayi, R. Chitra, and M. J. Rozenberg, Phys. Rev. B **73**, 041103(R) (2006).
[11] A. Macridin, M. Jarrell, and T. Maier, Phys. Rev. B **74**, 085104 (2006).
[12] Ph. Werner and A. J. Millis, Phys. Rev. B **75**, 085108 (2007).
[13] D. J. García, E. Miranda, K. Hallberg, and M. J. Rozenberg, Phys. Rev. B **75**, 121102(R) (2007).
[14] M. Eckstein, M. Kollar, M. Potthoff, and D. Vollhardt, Phys. Rev. B **75**, 125103 (2007).
[15] T. Pruschke, J. Keller, A. I. Poteryaev, I. A. Nekrasov, and V. I. Anisimov, J. Phys.: Condens. Matter **9**, 7359 (1997).
[16] M. B. Zolfl, T. Pruschke, J. Keller, A. I. Poteryaev, I. A. Nekrasov, and V. I. Anisimov, Phys. Rev. B **61**, 12810 (2000).
[17] K. Held, N. Blümer, A. I. Poteryaev, V. I. Anisimov, and D. Vollhardt, Eur. Phys. J. B **18**, 55 (2000).
[18] V. S. Oudovenko, G. Pálsson, S. Y. Savrasov, K. Haule, and G. Kotliar, Phys. Rev. B **70**, 125112 (2004); V. S. Oudovenko, G. Pálsson, K. Haule, G. Kotliar, and S. Y. Savrasov, *ibid.* **73**, 035120 (2006).
[19] L. Craco, M. S. Laad, S. Leoni, and E. Müller-Hartmann, Phys.

Rev. B **70**, 195116 (2004).
[20] E. Pavarini, S. Biermann, A. Poteryaev, A. I. Lichtenstein, A. Georges, and O. K. Andersen, Phys. Rev. Lett. **92**, 176403 (2004).
[21] G. Keller, K. Held, V. Eyert, D. Vollhardt, and V. I. Anisimov, Phys. Rev. B **70**, 205116 (2004).
[22] A. I. Poteryaev, J. M. Tomczak, S. Biermann, A. Georges, A. I. Lichtenstein, A. N. Rubtsov, T. Saha-Dasgupta, and O. K. Andersen, Phys. Rev. B **76**, 085127 (2007).
[23] V. I. Anisimov, I. A. Nekrasov, D. E. Kondakov, T. M. Rice, and M. Sigrist, Eur. Phys. J. B **25**, 191 (2002), and references therein; See also Z. Fang, N. Nagaosa, and K. Terakura, Phys. Rev. B **69**, 045116 (2004).
[24] V. A. Khodel, J. W. Clark, H. Li, and M. V. Zverev, Phys. Rev. Lett. **98**, 216404 (2007).
[25] A. Georges, G. Kotliar, W. Krauth, and M. J. Rozenberg, Rev. Mod. Phys. **68**, 13 (1996).
[26] M. Caffarel and W. Krauth, Phys. Rev. Lett. **72**, 1545 (1994).
[27] C. A. Perroni, H. Ishida, and A. Liebsch, Phys. Rev. B **75**, 045125 (2007); See also A. Liebsch, Phys. Rev. Lett. **95**, 116402 (2005); A. Liebsch and T. A. Costi, Eur. Phys. J. B **51**, 523 (2006).
[28] R. B. Lehoucq, D. C. Sorensen, and C. Yang, *ARPACK Users' Guide* (Society for Industrial and Applied Math, Philadelphia, 1997).
[29] A. Liebsch and H. Ishida, Eur. Phys. J. B (to be published).
[30] H. Ishida and A. Liebsch, Phys. Rev. B (to be published).
[31] E. Pavarini, A. Yamasaki, J. Nuss, and O. K. Andersen, New J. Phys. **7**, 188 (2005).
[32] M. W. Haverkort, Z. Hu, A. Tanaka, G. Ghiringhelli, H. Roth, M. Cwik, T. Lorenz, C. Schüßler-Langeheine, S. V. Streltsov, A. S. Mylnikova, V. I. Anisimov, C. de Nadai, N. B. Brookes, H. H. Hsieh, H.-J. Lin, C. T. Chen, T. Mizokawa, Y. Taguchi, Y. Tokura, D. I. Khomskii, and L. H. Tjeng, Phys. Rev. Lett. **94**, 056401 (2005), and references therein.